Complexes Self-Associate by Hydrogen Bonding and Metallophilic Attraction: Theoretical Study

FERNANDO MENDIZABAL,[1] DANA REYES,[1] CLAUDIO OLEA-AZAR[2]

[1]*Departamento de Química, Facultad de Ciencias, Universidad de Chile, Casilla 653, Santiago, Chile*

[2]*Departamento de Química Inorgánica y Analítica, Facultad de Ciencias Químicas y Farmacéuticas, Universidad de Chile, Casilla 233, Santiago 1, Chile*

ABSTRACT: Hydrogen bonding and metallophilic attractions are studied in the model systems: $[(AuNH_3Cl)_2]$, $[(AuNH(CH_3)_2Cl)_2]$, $[\{Au_2(\mu\text{-}SH)(PH_2O)(PH_2OH)\}_2]$, $[(CuNH_3Cl)_2]$, and $[\{Cu(NH_3)Cl\}_4]$ at the Hartree–Fock (HF) and second-order Møller–Plesset (MP2) levels. The two interactions are found to be comparable and prevailing in the final structure. It is determined that the aurophilic contact has a same magnitude that the hydrogen bonding, and is stronger than the cuprophilic interaction. The presence of hydrogen bond directs the growth of the crystal.

Key words: gold; copper; metallophilic

Introduction

There has been important progress in the design and synthesis of inorganic molecular material used as simple building blocks that can be induced to form complex molecular structures by self-assembly [1–5]. Recent experimental and theoretical work has discussed the known metallophilic and aurophilic interactions coexisting with hydrogen bonding (HB), M–π, or π–π attractions [6–8]. All these interactions can participate as building blocks in the supramolecular structures [9, 10].

For the case of the intermolecular interaction combination as metallophilic and hydrogen bonding have shown a strong directionality to control the supramolecular structures [11–14]. Some systems that have aurophilic and cuprophilic attraction coexisting with hydrogen bonding are shown in Table I. Theoretical models have demonstrated the importance both of their magnitude and of their comparable force [6, 7]. In general, the combination of metallophilic and other secondary binding interactions, such as hydrogen

Correspondence to: F. Mendizabal; e-mail: hagua@uchile.cl

Contract grant sponsor: FONDECYT (Conicyt-Chile).

Contract grant number: 1020141.

Contract grant sponsor: Millennium Nucleus for Applied Quantum Mechanics and Computational Chemistry (MIDEPLAN).

Contract grant number: P02-004-F.

TABLE I

Experimental values for metallophilic attraction and hydrogen bonding.[a]

System	M(I)–M(I)/pm	D–A/pm	A–H/pm	<A–M–M–A	Ref.
[(piperidine)AuCl]	330.1	334.6	244.6	150.5°	11
[(dicyclohexylamine)AuCl]	326.8	339.1	243.0	151.1°	11
[{Au_2(μ-SPh)(PPh_2O)(PPh_2OH)}$_2$]	307.3	241.0	155.1	58.4° [b]	12
[{Cu(NH_3)Cl}$_4$]	297.9	355.0	266.0	179.1°	13

[a] Distances in pm. Donor (D) and acceptor (A) atoms refer to the hydrogen bond.
[b] P–O· · ·O–P.

bonding, has immense potential in the design of molecular materials [1–10].

The cation metals that participate in the metallophilic attractions have d^8, d^{10} o, s^2 configurations [15]. These closed-shell interactions are estimated to be energetically similar to hydrogen bonds (20–50 kJ/mol) in the case of Au(I) and to be weaker for other metals, such as Ag(I), Cu(I), Tl(I), Hg(II), and Pt(II) [16]. At the theoretical level, the metallophilic and aurophilic attractions are interesting according to when the electronic correlation effects are accounted, strengthened by relativistic effects; this phenomenon can be noticeable [17–19]. Thus, the nature of these interactions can be studied by comparing calculations done at both Hartree–Fock (HF) and post-Hartree–Fock [i.e., second-order Møller–Plesset (MP2)] levels for a given model system. Hence, it is necessary to perform calculations at least at the MP2 level for a proper description of the dispersion forces (with additional allowance for virtual charge-transfer terms), which are included among the correlation effects [17]. In contrast, calculations based on density functional theory (DFT) on metallophilic attractions are not adequate due to the unreliable interaction energy near the van der Waals minimum, because the specific form of correlation energy (virtual double-dipole excitations, leading to an R^{-6} power law) is not properly described [20].

The aim of the present work is to study theoretically the intermolecular interaction of the type Au(I)–Au(I) and Cu(I)–Cu(I) in combination with hydrogen bonds, comparing each model at the HF and MP2 levels, thus allowing the correlation effects on the metal–metal and HB distance to be estimated.

Models and Method

For each model combining metallophilic attractions and hydrogen bonds, we have optimized the structural of monomers [$ClAuNH_3$], [ClAuNH-(CH_3)$_2$], [Au_2(μ-SH)(PH_2O)(PH_2OH)], and [ClCu(NH_3)] at the HF and MP2 levels. The phenylphosphine and dicyclohexyl ligands of the original experimental structures are thereby replaced by the phosphine and hydrogen or methyl groups, respectively. The monomer geometries are then used for studying the M· · ·M and hydrogen bonding intermolecular interactions in dimers **1–6** (Fig. 1). The interaction energy, $V(R)$, between the monomers was obtained including a counterpoise correction.

The Gaussian 98 package was used [21]. The gold and copper atoms were treated by a 19 valence-electron (VE) quasi-relativistic (QR) pseudopotential (PP) from Stuttgart [22]. The *f*-orbitals are necessary for the weak intermolecular interactions, as has been demonstrated previously for each atom. We employed two *f*-type polarization functions: Au(0.2, 1.19) and Cu(0.24, 3.70) [13]. This is desirable for a more accurate description of the interaction energy. Also, atoms C, N, O, P, and Cl were treated by the valence electrons for each atom, respectively [23]. For these atoms, double-zeta basis sets were used and one *d*-orbital polarization function was added. For the H atom, a double-zeta plus one *p*-type polarization function was used [24].

Results and Discussion

Table II reports the optimized distances and main parameters obtained for models **1–6** at the HF and MP2 levels. It can be noted that the structural parameters change substantially from the HF level to the MP2 level, in particular M· · ·M and hydrogen bonding distances. The usual correlation-induced shortening is found for all systems, suggesting the aurophilic attractions by models **1–4** and cuprophilic interactions by models **5** and **6**. At the HF level, the metallophilic attraction disappears, while substantial parts of the hydrogen bonding survive

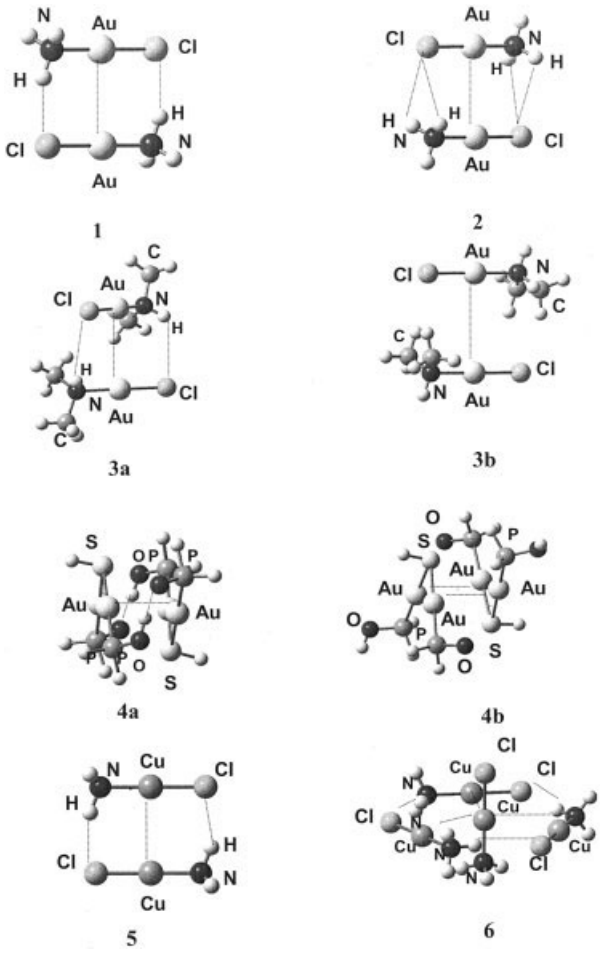

FIGURE 1. Theoretical models with and without hydrogen bonding: $[(AuNH_3Cl)_2]$ (**1,2**), $[(AuNH(CH_3)_2Cl)_2]$ (**3a,3b**), $[\{Au_2(\mu\text{-}SH)(PH_2O)(PH_2OH)\}_2]$ (**4a,4b**), $[(CuNH_3Cl)_2]$ (**5**), and $[\{Cu(NH_3)Cl\}_4]$ (**6**).

(only a part of the hydrogen bonding coming from the dispersion). The optimized interaction energies $V(R_e)$ are also shown in Table II. The potential curves are given in Figures 2–5.

Of the models proposed, **1**, **2**, **3a**, **4a**, **6**, and **5** have hydrogen bonds, while **3b** and **4b** do not have a hydrogen bond. The change is obtained by rotating the —$NH(CH_3)_2$ and —$PH_2(OH)$ groups through 120°, respectively. Furthermore, the average dihedral angle A–M–M–A was allowed to seek minimal energy. This value has also been reproduced by our calculations when compared with the experimental value (see Tables I and II).

An estimate of the intermolecular metallophilic attraction energy can be obtained from the difference between the MP2 energies of each model at HF- and MP2-optimized geometries at the equilibrium distance of MP2, thus sampling a part of the metallophilically induced stabilization. The results are shown in Table III.

$[(AuNH_3Cl)_2]$ (1,2)

In **1** and **2**, there are one and two HB per –Cl, respectively. The gold–gold distance at the HF and MP2 levels is very similar for both models, but the donor–acceptor (D–A) distance is shorter in **1** than in **2**. Thus, we can appreciate that the HB is stronger in the first model. From the interaction-energy curves obtained (see Table III), the aurophilic interaction is 29.7 and 30.7 kJ/mol per pair by **1** and **2**, respectively. They are found in the classic range of this interaction. The hydrogen bond energy pair Cl···H—N are 30.3 and 12.8 kJ/mol by **1** and **2**, respectively. This difference, more than double between **1** and **2**, is due to the shortest distance of the HB in **1** and thus has a greater force in the same measure.

$[(AuNH(CH_3)_2Cl)_2]$ (3a,3b)

We have used a similar model to **2**, changing two —H by two —CH_3 groups. The objective is to reproduce the experimental structures [(piperidine)AuCl] and [(dicyclohexylamine)AuCl]. In **3a**, analogous trends are found with respect to **2**, but the Au–Au distance is now shorter. The hydrogen bonding is comparable at the experimental structures. For the Cl···H—N HB in **3a**, the energy at the HF level is 12.3 kJ/mol per bond. The remaining estimate for the aurophilic energy is 50.1 kJ/mol, at the upper end of the typical range. This must be to the short Au–Au distance. The MP2 calculation reproduces the experimental results, while at the HF level an increase is observed in the Au···Au distance (repulsion). This last produces an increase in the remaining parameters with a weakening of the HB. Furthermore, the dihedral angle Cl–Au–Au–Cl is reproduced at the HF and MP2 levels respect of the experimental value [11]. This is indicative of the direction that takes the force of the HB.

Model **3b** is obtained through a rotation of the —$NH(CH_3)_2$ groups. Thus, hydrogen bonding is eliminated in model **3a**. We can appreciate that the Au–Au distance increase to values on 400 pm at the HF and MP2 levels. The —CH_3 produces a repulsion effect on the —Cl atoms that it must be greater to the aurophilic attraction. The dihedral angle Cl–Au–Au–Cl is 180°, distant to the experimental value of 151.1° in [(dicyclohexylamine)AuCl] [11], which demonstrates the importance of the HB in the growth of the crystal.

TABLE II

Optimized M–M distances and hydrogen-bonding geometries for complexes at the HF and MP2 levels.*

Model	Method	M–M	D–A	H–A	<A–M–M–A	$V(R_e)$
$[(AuNH_3Cl)_2]$ **1**	MP2	328.8	329.5	233.9	180°	−90.3
	HF	352.3	352.9	257.3	180°	−66.2
$[(AuNH_3Cl)_2]$ **2**	MP2	323.7	234.4	288.5	180°	−81.4
	HF	353.1	353.7	316.7	180°	−57.5
$[(AuNH(CH_3)_2Cl)_2]$ **3a**	MP2	314.1	338.1	274.4	146.6°	−74.6
	HF	366.9	387.7	325.9	145.5°	−37.3
$[(AuNH(CH_3)_2Cl)_2]$ **3b**	MP2[a]	436.8	437.2	—	180°	−50.1
	HF[a]	454.1	454.4	—	180°	−33.6
$[\{Au_2(\mu\text{-SH})(PH_2O)(PH_2OH)\}_2]$ **4a**	MP2	296.1	249.6	154.4	55.4° [b]	−273.9
	HF	327.8	256.9	165.2	51.7° [b]	−231.8
$[\{Au_2(\mu\text{-SH})(PH_2O)(PH_2OH)\}_2]$ **4b**	MP2[a]	312.6	559.7	—	145.9° [b]	−110.5
	HF[a]	411.0	580.3	—	146.1° [b]	−41.0
$[(CuNH_3Cl)_2]$ **5**	MP2	333.9	334.4	229.4	180°	−78.4
	HF	348.3	348.7	239.3	180°	−76.9
$[\{Cu(NH_3)Cl\}_4]$ **6**	MP2	329.5	374.3	274.3	180°	−23.5
	HF	335.1	385.3	298.3	180°	−8.7

* Distances in pm. Interaction energies, $V(R_e)$, in kJ/mol. Donor (D) and acceptor (A) atoms refer to the hydrogen bond.
[a] Without hydrogen bond.
[b] P–O· · ·O–P.

$[\{Au_2(\mu\text{-SH})(PH_2O)(PH_2OH)\}_2]$ (4a,4b)

This model shows intra- and intermolecular aurophilic interactions. We center our attention on the intermolecular interactions through HB and on the aurophilic attraction for the pair of opposite A-frames. Of these models, **4a** does, and **4b** does not, have hydrogen bonds. Better results (see Table II), compared with the experimental structure $[\{Au_2(\mu\text{-SPh})(PPh_2O)(PPh_2OH)\}_2]$ [12], are found for system **4a** with Au–Au = 296.1 pm, O· · ·O (D–A) = 249.9 pm, and H· · ·O = 154.4 pm distances at the MP2 level. The

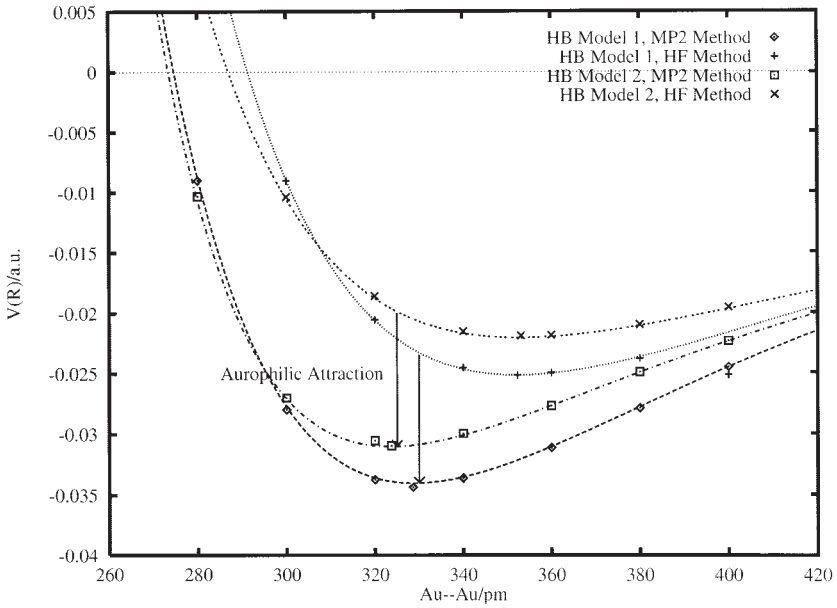

FIGURE 2. Interaction energies $V(R)$ at the HF and MP2 levels for models **1** and **2**.

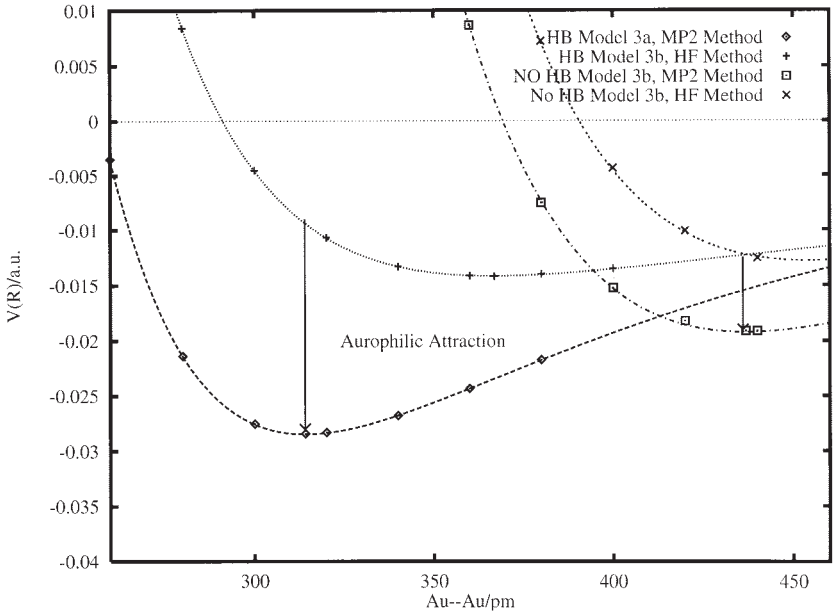

FIGURE 3. Interaction energies $V(R)$ at the HF and MP2 levels for models **3a** and **3b**.

dihedral angle P–O· · ·O–P is reproduced at the experimental value. When we compare the experimental compound and model **4a**, the intermolecular Au· · ·Au distances are considerably shorter and indicate a much stronger aurophilic attraction among these atoms. Furthermore, the groups combine intermolecularly by P–O· · ·H–O–P bonding, the distances between oxygen atoms O· · ·O are within the range that is considered diagnostic of strong hydrogen bond.

At the MP2 level, the energy minimum is R_e = 296 pm and $V(R_e)$ = −273 kJ/mol. This energy includes an estimate for both the hydrogen bonds and the aurophilic attractions. The latter contribution is 34.5 kJ/mol per contact, while the contribution per hydrogen bond is 102.6 kJ/mol.

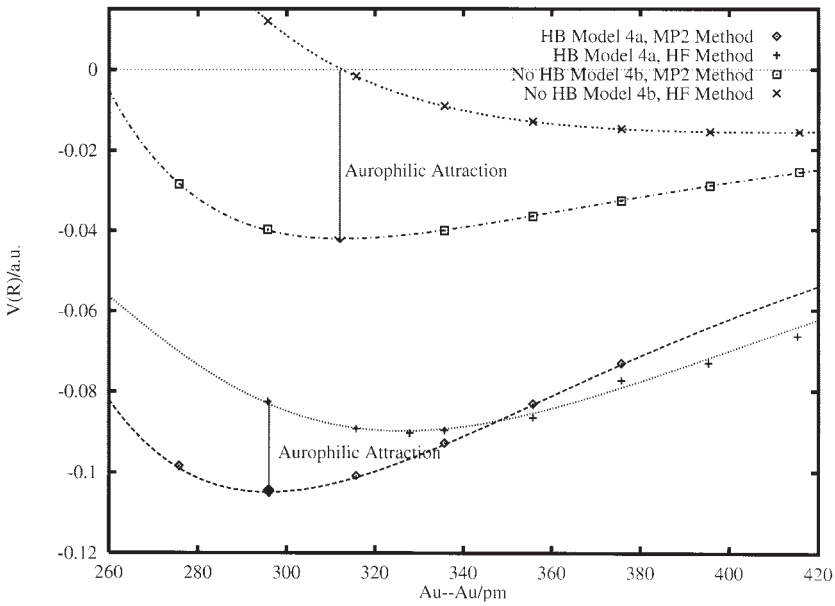

FIGURE 4. Interaction energies $V(R)$ at the HF and MP2 levels for models **4a** and **4b**.

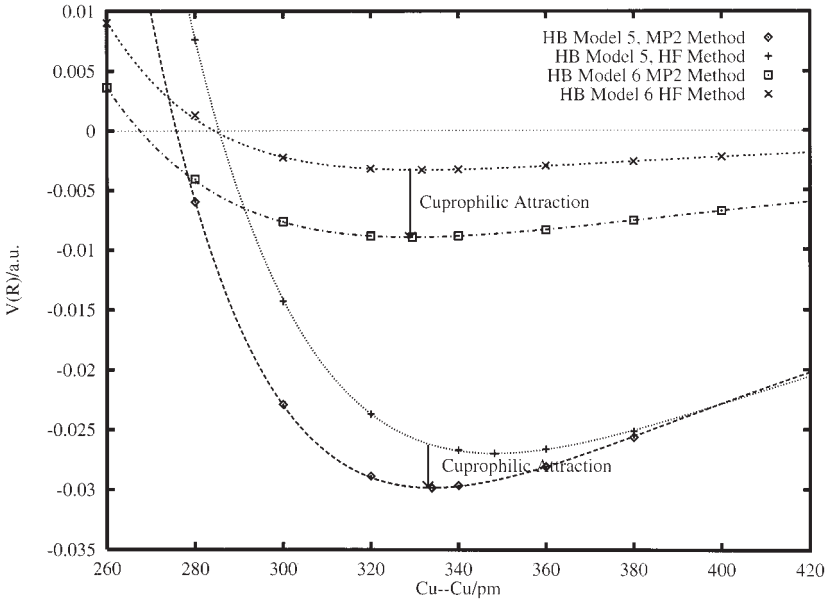

FIGURE 5. Interaction energies $V(R)$ at the HF and MP2 levels for models **5** and **6**.

The established hydrogen bond presents a high magnitude (102.6 kJ/mol). This can be explained by the fact that the O···H—O distance is short, 154.4 pm and, additionally, the donor and acceptor atoms are oxygens. In this case, we can speak of short strong hydrogen bonds (SSHBs). SSHBs have attracted a great deal of interest during the past few years [25, 26]. Experimental and theoretical studies have confirmed that the force of the SSHBs are within the range of 100–120 kJ/mol. Thus, we have a dimer of A-frames with high nucleation and inter-SSHBs.

For the model without HB (**4b**), we obtain a mild, longer equilibrium Au–Au distance of 312.6 pm with a smaller interaction energy of 30.8 kJ/mol per contact (see Table III) at the MP2 level, while at the HF level, there is no evident minimum. The interaction potential in Figure 4 is negative due to an electrostatic and induction contributions would still be there.

$[(CuNH_3Cl)_n]$ $(n = 2, 4)$ (5,6)

These models are one of the few systems published recently, providing evidence of Cu(I)–Cu(I) attractive interactions in the absence of any bridging ligand [13]. Model **5** is a classic dimer with copper contacts and hydrogen bonds, an analogue

TABLE III

Metallophilic interaction energies [Δ*E*(MP2–HF)], metal–metal energy per pair [Δ*E*(M–M)], and hydrogen bond energy [Δ*E*(HB)] per pair.*

Model	M–M	Δ*E*(MP2–HF)	Δ*E*(M–M)	Δ*E*(HB)
$[(AuNH_3Cl)_2]$ **1**	328.8	−29.7	−29.7	−30.3
$[(AuNH_3Cl)_2]$ **2**	323.7	−30.3	−30.3	−12.8
$[(AuNH(CH_3)_2Cl)_2]$ **3a**	314.1	−50.1	−50.1	−12.3
$[(AuNH(CH_3)_2Cl)_2]$[a] **3b**	436.8	−18.0	−18.0	—[a]
$[\{Au_2(\mu\text{-}SH)(PH_2O)(PH_2OH)\}_2]$ **4a**	296.1	−68.9	−34.5	−102.6
$[\{Au_2(\mu\text{-}SH)(PH_2O)(PH_2OH)\}_2]$[a] **4b**	312.6	−61.5	−30.8	—[a]
$[(CuNH_3Cl)_2]$ **5**	333.9	−9.37	−9.37	−35.5
$[\{Cu(NH_3)Cl\}_4]$ **6**	329.5	−14.83	−4.9	−4.2

* Distance in pm and energy in kJ/mol.
[a] Without hydrogen bond.

at the model **1**. In model **6**, each copper atom is surrounded by three other [Cu(NH_3)Cl] moieties, leading to a triginal–bipyramidel coordination sphere [13]. At the MP2 level, the Cu···Cu contact distances are 333.9 pm and 329.5 pm (Table II) by **5** and **6**, respectively. In both models, the Cu···Cu distance is longer than the experimental average value of 297.9 pm (see Table I). The D–A and H–A distances are very close to experimental. In this case, hydrogen bonding is of type Cl···H–N, which is longer than in models **1** and **2**.

In contrast, at the HF level, all distances are lengthened, since the dispersion effect disappears. Thus, the hydrogen bond is maintained. We estimate the cuprophilic interaction as the difference of the MP2 and HF energies at the equilibrium distance. The cuprophilic contacts per pair are 9.4 and 4.9 kJ/mol by **5** and **6**, respectively. The described magnitudes are comparable to that reported by Schwertfeger and colleagues [27] in model dimers of the type $[CH_3CuX]_2$ (X = OH_2, NH_3, SH_2, PH_3, N_2, CO, CS, CNH, CNLi) and by Alvarez and colleagues [28] in $[Cu(NH_3)Cl]_2$ [28] at the MP2 level.

The hydrogen binding contribution amounts to 35.5 and 4.2 kJ/mol per HB, respectively (see Table III). Thus, the magnitude of the HB is equal to, or greater than, the cuprophilic interaction, directing the type of final structure that adopts the crystal.

References

1. Hollatz, C.; Schier, A.; Schmidbaur, H. J Am Chem Soc 1997, 119, 8115.
2. Hao, L.; Mansour, M. A.; Lachicotte, R. J.; Gysling, H. J.; Eisenberg, R. Inorg Chem 2000, 39, 5520.
3. Tzeng, B.-C.; Schier, A.; Schmidbaur, H. Inorg Chem 1999, 38, 3978.
4. Bachman, R. E.; Fioritto, M. S.; Fetics, S. K.; Cocker, T. M. J Am Chem Soc 2001, 121, 5376.
5. Mohr, F.; Jennings, M. C.; Puddephatt, R. Angew Chem Int Ed 2004, 43, 969.
6. Codina, A.; Fernández, E. J.; Jones, P. G.; Laguna, A.; López-de-Luzuriaga, J. M.; Monge, M.; Olmos, M. E.; Pérez, J.; Rodríguez, M. A. J Am Chem Soc 2002, 124, 6781.
7. Mendizabal, F.; Pyykkö, P.; Runeberg, N. Chem Phys Lett 2003, 370, 733.
8. Zhang, I.-P.; Wang, Y.-B.; Huang, X.-C.; Lin, Y.-Y.; Chen, X.-M. Chem Eur J 2005, 11, 552.
9. Hunks, W. J.; Jennings, M. C.; Puddephatt, R. J. Inorg Chem 2002, 41, 4590.
10. Ganguly, S.; Chattopadhyay, S.; Sinha, C.; Chakravorty, A. Inorg Chem 2000, 39, 2954.
11. Ahrens, B.; Jones, P. G.; Fischer, A. K. Eur J Inorg Chem 1999, 1103.
12. Hunks, W. J.; Jennings, M. C.; Puddephatt, R. J. Inorg Chem 2000, 39, 2699.
13. Margraf, G.; Bats, J. W.; Bolte, M.; Lerner, H.-W.; Wagner, M. Chem Commun 2003, 956.
14. Hollatz, C.; Schier, A.; Riede, J.; Schmidbaur, J. Chem Soc Dalton Trans 1999, 111.
15. Pyykkö, P. Chem Rev 1997, 97, 597.
16. Pyykkö, P. Angew Chem Int Ed 2004, 43, 4412.
17. Pyykkö, P.; Runeberg, N.; Mendizabal, F. Chem Eur J 1997, 3, 1451.
18. Pyykkö, P.; Mendizabal, F. Chem Eur J 1997, 3, 1458.
19. Mendizabal, F.; Zapata-Torres, G.; Olea-Azar, C. Chem Phys Lett 2003, 382, 92.
20. Pyykkö, P. Angew Chem Int Ed 2002, 41, 3573.
21. Frisch, M. J.; Trucks, G. W.; Schlegel, H. B.; Gill, P. M. W.; Johnson, B. G.; Robb, M. A.; Cheeseman, J. R.; Keith, K. T.; Petersson, G. A.; Montgomery, J. A.; Raghavachari, K.; Al-Laham, M. A.; Zakrzewski, V. G.; Ortiz, J. V.; Foresman, J. B.; Cioslowski, J.; Stefanov, B. B.; Nanayakkara, A.; Challacombe, M.; Peng, C. Y.; Ayala, P. Y.; Chen, W.; Wong, M. W.; Andres, J. L.; Replogle, E. S.; Gomperts, R.; Martin, R. L.; Fox, D. J.; Binkley, J. S.; Defrees, D. J.; Baker, J.; Stewart, J. P.; Head-Gordon, M.; Gonzalez, C.; Pople, J. A. Gaussian 98; Revision A.11; Gaussian: Pittsburgh, PA, 2002.
22. Andrae, D.; Haeussermann, U.; Dolg, M.; Stoll, H.; Preuss, H. Theor Chim Acta 1990, 77, 12.
23. Bergner, A.; Dolg, M.; Küchle, W.; Stoll, H.; Preuss, H. Mol Phys 1993, 80, 1431.
24. Huzinaga, S. J Chem Phys 1965, 42, 1293.
25. Kim, Y.; Lim, S.; Kim, Y. J Phys Chem A 1999, 103, 6632.
26. Pacios, L.; Gómez, P. C. J Phys Chem A 2004, 108, 11783.
27. Hermann, H. L.; Boche, G.; Schwerdtfeger, P. Chem Eur J 2001, 7, 5333.
28. Liu, X.-Y.; Mota, F.; Alemany, P.; Novoa, J. J.; Alvarez, S. Chem Commun 1998, 1148.